



Open Archive Toulouse Archive Ouverte


OATAO is an open access repository that collects the work of Toulouse researchers and makes it freely available over the web where possible

This is an author's version published in: <http://oatao.univ-toulouse.fr/25765>

Official URL:

<https://doi.org/10.1007/s10652-019-09720-x>

To cite this version:

Cassan, Ludovic and Roux, Hélène  and Dartus, Denis
Velocity distribution in open channel flow with spatially distributed roughness. (2019) Environmental Fluid Mechanics.
ISSN 1567-7419.

Any correspondence concerning this service should be sent to the repository administrator: tech-oatao@listes-diff.inp-toulouse.fr

Velocity distribution in open channel flow with spatially distributed roughness

Ludovic Cassan¹  · H  l  ne Roux¹ · Denis Dartus¹

Abstract

A numerical procedure is proposed to estimate the velocity distribution in open channel flow, for engineering applications. A method based on the mixing length model and sub-division of the wetted surface, is modified to easily integrate a lateral distribution of roughness. Several friction models for vegetated or rough flows can be added, two of which have been tested. The numerical procedure was developed with a commercial software (Matlab) to ensure fast computation and possible coupling with 1D hydraulic models. The validation of the computation has been done with rectangular and compound channels with spatially distributed roughness. The usefulness of the method for ecohydraulics is demonstrated with two applications: box culvert design for fish passes and 1D modelling of mountain river flows for which experimental results from a laboratory scale-model is compared to predictions. The interest of a friction law calibrated with a real grain roughness size is put forward.

Keywords Roughness · Numerical modelling · Velocity distribution · Fish pass · Mountain river

1 Introduction

The computation of the velocity distribution in an open channel often needs a CFD method to take into account all the processes involved in fluid mechanics. For instance, an efficient turbulence model is necessary to well compute secondary flows which can modify velocities in the region under the free surface. The turbulence is also significant for overbank flows occurring during flood events and for which the momentum transfer is crucial in the computation of velocity in the compound channel [33]. Nevertheless the use of a full 3D

✉ Ludovic Cassan
lcassan@imft.fr

H  l  ne Roux
helene.roux@imft.fr

Denis Dartus
denis.dartus@imft.fr

¹ Institut de M  canique des Fluides de Toulouse (IMFT), Universit   de Toulouse, CNRS, Toulouse, France

model for river is limited to specific flows where other methods are clearly unsatisfactory. For engineering studies, a preliminary estimate of the velocity distribution can be helpful for vegetated flow or laterally distributed roughness, but also to predict erosion process or aquatic habitat. As the flow is mainly bed driven, a method which takes into account an accurate description of the bed friction could be an effective tool. The most common way to distribute the flow over a cross section is the Einstein method which only provides a velocity averaged on the vertical direction [8]. This method is attractive because it is analytical. Hence, it could describe the velocity distribution consecutively at a 1D computation performed with an averaged value of discharge in the main channel and overbanks. Improvements of this method have been proposed for rectangular channel. It estimates the bed shear stress and then enhances the computation of sediment transport [11]. The 2D shallow water modelling also takes into account the lateral distribution of roughness or cross section shape. But, the model still provides only depth-averaged velocity and secondary currents are not computed even if they influence the hydrodynamics [31]. This paper is devoted to investigate, present and validate a methodology that predicts vertical distribution of longitudinal velocity with a non uniform transversal distribution of roughness and complex geometry. This method brings accuracy on velocity prediction for sediment transport, network management [2], flow measurements but also aquatic habitat and fish passage design [35]. It can be used for streambank stability studies or channel design. The calculation is based on the method from Kean et al. [14]. It was chosen because it seems to be more physically-based than alternative methods [22]. Indeed, the method from Maghrebi and Rahimpour [22] considers an exponential velocity distribution and a calibration coefficient which is not directly related to the roughness height k . Here, with respect to Kean et al. [14] method, the possibility to use several formulations of the friction law has been added in order to integrate novel studies on this subject [1, 12, 13, 30] and the computational time has been improved using some approximations specified in Sect. 2.1.

In a first step, the model is detailed focusing on the new aspects concerning boundary conditions and friction laws. Secondly, the model is validated with experiments conducted at the Institute of Fluid Mechanics in Toulouse and for simple geometries (rectangular) for which experimental results are well-known in literature [24, 36] (smooth and rough velocity profile, shear stress partitioning between sidewall/bed). The method ability to predict the velocity field in the presence of non-uniform lateral roughness is demonstrated by comparison with the results from Kean et al. [14] and Wang et al. [34]. Finally the application of the method is presented for typical engineering issues to point out its advantages in comparison with equivalent methods. These examples focus on benefits for prediction of flow area with ecological interest, extrapolation of surface velocity measurements, design of structure with laterally distributed roughness or erosion/deposition process at river banks.

2 Theoretical background

2.1 Equations

The velocity in an open channel is mainly bed driven which enables relevant prediction of the stage-discharge relationship: Manning law or more complicated model for vegetation or macro-roughness bed [9, 13, 27]. As a consequence, in most of cases, a good calculation of the velocity gradient near the bed is sufficient to produce a satisfactory value of the discharge. A turbulence model based on a mixing length has shown its efficiency if this length depends

linearly on the distance of the wall. Considering these observations, several authors tried to estimate the spatial repartition of velocity [4, 14, 22]. It is considered that the most pertinent model is the one from Kean et al. [14] because it is related to a turbulent process and momentum balance. The two dimensional equations for longitudinal velocity, u , is solved for a steady flow (Eq. 1). Assuming that the transversal and vertical velocities are neglected, the Navier-Stokes equation is written as follows :

$$\rho u \frac{\partial u}{\partial x} = -\frac{\partial p}{\partial x} + \rho g S_0 + \frac{\partial}{\partial y} \left(\rho \nu_t \frac{\partial u}{\partial y} \right) + \frac{\partial}{\partial z} \left(\rho \nu_t \frac{\partial u}{\partial z} \right) \quad (1)$$

with x, y, z respectively the longitudinal, transverse and vertical coordinates, ν_t the turbulent viscosity, p the pressure, the slope $S_0 = -dz_b/dx = \tan(\theta) \approx \sin(\theta)$ where z_b is the bed level and θ is the angle of the bed with the horizontal line. If the pressure distribution normal to the bed is considered hydrostatic, the pressure term is expressed as a function of the waterdepth. Moreover a strong assumption is to substitute the advective term $u \frac{\partial u}{\partial x}$ with averaged term obtained by the area integration (V is the averaged velocity). The advantage is to get an expression similar to shallow water model but with a friction term that could take into account the lateral distribution of roughness. However, this substitution doesn't reproduce the influence of the advective term on the velocity profile, especially near the bed where the advective term tends to 0. The Eq. 1 becomes :

$$0 = -g \frac{\partial h}{\partial x} + g S_0 - \frac{1}{2} \frac{\partial V^2}{\partial x} + \frac{\partial}{\partial y} \left(\nu_t \frac{\partial u}{\partial y} \right) + \frac{\partial}{\partial z} \left(\nu_t \frac{\partial u}{\partial z} \right) \quad (2)$$

In the Eq. 2, the integration of the turbulent term is responsible for the energy dissipation which is equal to the head loss ($d(h + z_b + V^2/2g)/dx$). As a consequence, the method from Kean et al. [14] based on the uniform flow assumption is here applied for gradually varied flow (with S_f the friction slope).

$$0 = g S_f + \frac{\partial}{\partial y} \left(\nu_t \frac{\partial u}{\partial y} \right) + \frac{\partial}{\partial z} \left(\nu_t \frac{\partial u}{\partial z} \right) \quad (3)$$

The turbulent viscosity is modelled with the Boussinesq assumption and a mixing length model. Unlike the model proposed by Kean et al. [14], the proposed model is calculated with the distance from the nearest wall instead of the length along the normal line to iso-velocity lines (isovels). This choice is made to ease numerical procedures and improve computational time.

$$\nu_t = l_m^2 \frac{\partial u}{\partial l} = l_m^2 \sqrt{\left(\frac{\partial u}{\partial y} \right)^2 + \left(\frac{\partial u}{\partial z} \right)^2} \quad (4)$$

where l_m is the mixing layer used for the computation of the turbulent viscosity.

$$l_m = \kappa d_w + l_0 \quad (5)$$

where κ is the von Karman constant, d_w is the distance from the boundary and l_0 the mixing length at the top of roughness. As the aim of the method is to integrate several kinds of boundary conditions, it is possible to describe them with the 3 conditions described hereafter. They are based (except smooth boundary) on the description of a turbulent boundary layer.

$$u_k = \frac{u_*}{\kappa} \ln \left(\frac{z-d}{z_0} \right) \quad (6)$$

with u_* the shear velocity, d the displacement height and z_0 the hydraulic roughness. The value of d depends on the roughness arrangement and size. The value is chosen to be consistent with the study of Cassan et al. [3] (macro-roughness) and Nikora et al. [25] (vegetation) which both propose a scaling length at the top of canopy $l_0 \approx 0.15 k$ where k is the roughness height. The computation of the turbulent viscosity at the top of canopy leads to $l_0 = \kappa(1 - d)k$. Therefore the displacement height d is assumed to be equal to $0.63 k$.

2.1.1 Smooth condition: BC1

When the flow is detected as being smooth at the boundary ($k^+ = \kappa u_* / \nu < 20$), the boundary velocity is computed with the Eq. 7, $z = z + t_{mesh}$, $l_0 = 0$ (Fig. 1), where t_{mesh} is the mesh size at the boundary.

$$u_k = u_* \left(\frac{1}{\kappa} \ln \left(\frac{t_{mesh} u_*}{\nu} \right) + 5.5 \right) \quad (7)$$

When k^+ ranges between 20 and 90, the functions from Ligrani and Moffat [19] are used. These functions allows reproducing as best as possible the wall friction whatever the flow regime smooth, transitional or rough.

2.1.2 From Nikuradse's formula: BC2

Considering Eq. 6, the parameters d and z_0 may vary with the arrangement of vegetation [21, 23] or macro-roughness [3, 29]. As they are responsible for the velocity profile near the bed, they must be predicted accurately. To be consistent with results on sand [26], we impose a hydraulic roughness height $z_0 = 0.033 k$. This value is the most commonly used for hydraulically rough bed and have been validated for a large range of flow. It is mostly pertinent when the water depth is high with respect to k . For example, this parametrization (in the integral form) is used in the modelling softwares HEC-RAS (1D) and Telemac (2D) in which the friction term can be defined as a function of the water depth.

2.1.3 From analytical resolution of the velocity within the roughness element: BC3

To take into account the flow within the roughness, the momentum equation could be solved considering drag force and turbulent terms [16]. Several studies used this method to compute the velocity distribution with vegetation or macro-roughness [1, 6, 13]. The

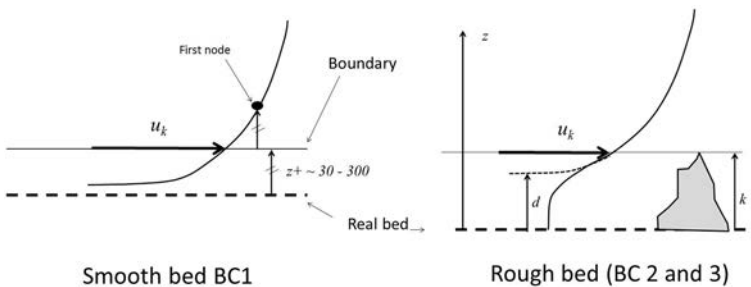


Fig. 1 Boundary conditions as a function of the flow regime

assumption of a logarithmic law above the roughness provides the values of d and z_0 which are needed to compute the boundary condition u_k at the top of canopy. Here, the approximation for rough and dense roughness layer from Cassan et al. [3] is tested. But the methodology can be applied using other analytic formulations. For instance, Katul et al. [13] suggests to use the experimental correlation $u_k/u_* = 3$ for dense vegetation, where l_0 is given by a canopy length scale. The law of Cassan et al. [3] for dense and gravel elements is incorporated with the following parameters $C_d = 0.7$ (drag coefficient), $k/D = 0.5$ (D is the gravel diameter), $C = 0.6$ (density area). An approximation of the velocity at the top of canopy is given :

$$\left(\frac{u_k}{u_*}\right) \approx \left(\frac{4k}{l_0}\right)^{1/3} \left(\frac{D(1-\sigma C)}{kC_d C}\right)^{1/3} \quad (8)$$

In Cassan et al. [3], the authors have shown that their model calibrated with the d_{84} of the bed granulometry should be similar to the friction law from Limerinos [20] which is validated and relevant for river flow.

2.2 Computational method

The numerical procedure is developed with scripts already existing in the Matlab Toolbox dedicated to the resolution of partial differential equations (PDE) with finite elements method. All scripts are freely available on request.

The cross section is meshed with triangular elements with a constant mesh size (t_{mesh}). Afterward, the mesh is refined only near the bed (Fig. 2) to reduce the computational time. For smooth flow, the minimum size should ensure that the distance between a first node and a boundary allows verifying the condition $30 \leq (z+ = u_*z/\nu) \leq 100$ where ν the molecular viscosity. For rough flow, the mesh can be larger and a maximum value of $h/30$ is used. To start the PDE resolution an initial condition is given by considering a constant velocity deduced from the Manning equation with $n = 0.025$. In a first step, the equation is solved with an uniform shear stress based on the hydraulic radius ($u_{*0} = \sqrt{gS_f R_h}$). The boundary condition at the free surface is a slip condition which leads to a maximum velocity at the free surface. Although in practical case, the secondary currents involve a dip phenomenon, this present model does not solve this issue because the applications studied here are focused on boundary layer. For wall boundaries, the velocity u_k is imposed considering the shear stress u_{*0} . The Eq. 3 is numerically solved with the Partial Differential Equation Toolbox using a Finite Element Method. The velocity distribution is then used to

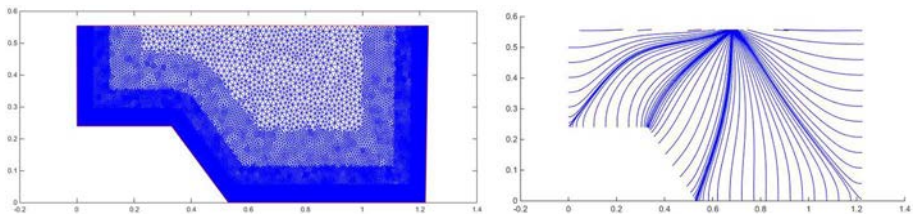


Fig. 2 Mesh used for the experimental case (left). Ray normal to isovel corresponding to the geometry from Kean et al. [14] (right)

compute the normal lines (ray) to isovels. These lines start from the boundary, and are spaced with a constant length t_{mesh} (or larger to reduce computation time) (Fig. 2). By applying the momentum balance to each sub-area A , it is possible to distribute the shear stress on the boundary lengths (P). Indeed the shear stress on the lateral ray is equal to 0 since the velocity gradient is null normal to this line. The value of u_* is given by the momentum balance considering a constant friction slope ($u_* = \sqrt{gS_f \frac{A}{P}}$). If the isovels are assumed to be horizontal, the method is equivalent to the Einstein method [8] which is the case for large river. In addition to providing vertical distribution, the advantages of Kean et al. [14] method mainly appears for rivers during low-flow periods (complex cross section) and narrow channels (irrigation and waste networks). Unlike the Einstein method, it is possible to consider the lateral boundary layer due to friction of vertical sidewalls. A second step consists in recomputing the velocity fields with a boundary condition u_k deduced from the shear velocity u_* obtained in the previous step. Several iterations with an adjusted relaxation constant are needed. The computation is stopped when a maximum number of iterations is reached (10) or if the residual criteria is smaller than 0.01. The computation lasts between 1 and 20 seconds depending on the section size and hydraulic conditions which impose the mesh size.

3 Experiments

As already mentioned, the method is relevant for natural cross section in particular if the channel can be considered as narrow, if the transverse roughness is quite heterogeneous or if specific frictions law are need. This kind of flow is typically encountered in mountainous rivers. Here, investigations are carried out with a scale model to focus on the influence of friction laws. Experiments were conducted in a tilting flume (1 m wide and 7 m long) at the Institute of Fluid Mechanics in Toulouse. A trapezoidal section was installed and covered with 2.5 cm pebbles (mean grain diameter) (Fig. 3). For slopes of 0.7, 1.2 and 1.7% and flow rates of 15.9, 22.6 and 41.2 l/s, the water depth at the centerline is measured with a point gauge at 4 m from the upstream end. In the result part it is checked that the application of the redistribution method should reproduce the measured stage-discharge relationship and predict the evolution of the friction as a function of the water depth. Indeed, the Manning equation generates a Manning coefficient n varying from 40%: n varies from 0.03 to 0.044 (Table 1).

The experiments were completed with the surface velocity measurement for 5 additional cases ($Q = 20$ and 50 l / s and $S = 0.5, 1$ and 2%). The method chosen is similar to Large Scale Particle Velocity Tracking (LSPTV) [32]. Floating balls with a 1 cm diameter were randomly distributed over the free surface and their trajectory were recorded with a fast camera (resolution $2K \times 2K$, 300 frames per second). More than 2000 images are captured for each experiment. The picture are thresholded considering their pixels intensity and the particules detected are deleted if their length is superior to 50% of the mean diameter (1 cm). The used algorithm is detailed in Ducrocq et al. [7], and the images were rectified with an homography matrix [28]. An example of the picture and the associated velocity vectors is given on Fig. 4. The final velocity field is reconstructed by gathering all data in the same cell (64×64 pixels) (Fig. 4).



Fig. 3 Experimental device and roughness

Table 1 Experimental results

S	Q	h	n
m/m	(l/s)	(m)	
0.007	22.6	0.099	0.037
0.012	22.6	0.089	0.041
0.017	22.6	0.083	0.044
0.007	15.9	0.085	0.042
0.012	15.9	0.078	0.047
0.017	15.9	0.073	0.051
0.007	41.2	0.126	0.030
0.012	41.2	0.116	0.035
0.017	41.2	0.109	0.037

4 Validation of the numerical procedure

The validation of the numerical procedure is performed with 4 different type of experiments to explore several flow conditions where the procedure is pertinent compared to Einstein’s method or Computational Fluid Mechanics considered as time consuming. We focus on:

- Rectangular channel to validate the implementation of boundary condition.
- Experiments described in previous part to emphasize the interest to use an adequate friction law, in particular for low submergence flow.
- The experiments from Kean et al. [14] to illustrate a strong spatially distributed roughness and its implication on the velocity field.

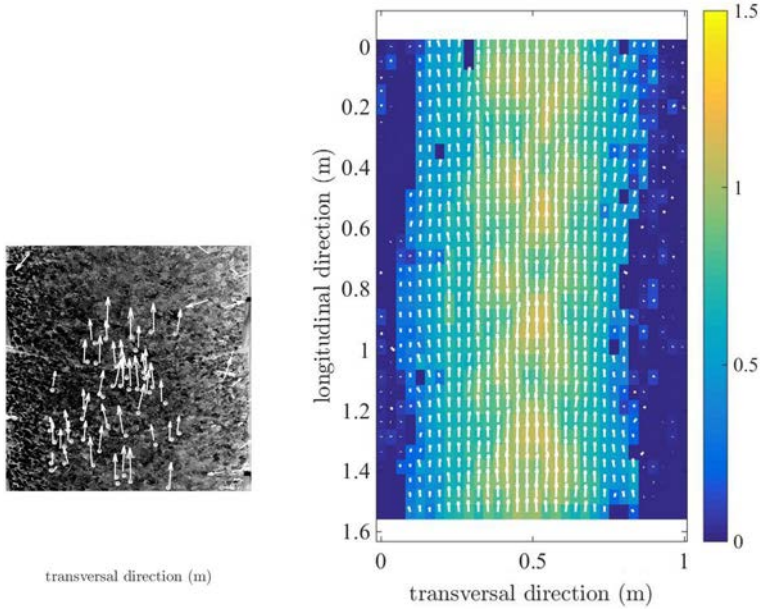


Fig. 4 Recorded image and particle detected (left) and velocity field (m/s) for $Q = 50$ l/s and $S = 1\%$ (right)

- The experiments from Wang et al. [34] with both a distributed roughness and a narrow open channel.

4.1 Rectangular channel

As the velocity field is concerned, the numerical procedure is firstly validated by considering the simple case of a rectangular channel with a constant roughness. The objective is to ensure that the computation provides logarithmic profiles depending on the roughness height. The computations were performed for $h/B = 0.1, 0.15, 0.2, 0.5, 1, 1.5, 2$ with a constant width $B = 1$ m.

The Fig. 5 shows that for all runs, the velocity profile is consistent with the logarithmic law near the bed. Mesh dependency study has proved that the velocity profiles are not modified if $t_{mesh} \leq l_0$ or $z_+ < 300$ for smooth cases. This boundary condition involves long computation time for a uniform mesh that is why a refinement is needed near the wall. In the upper region, the velocity is lower than the log-law profile unlike an empirical turbulent wall-bounded flow. The method is not able to reproduce a velocity higher than the logarithmic law because the slip condition imposes a zero-gradient at the free surface. For real flow, the higher velocity is due to both secondary currents and variation of the turbulent properties which are not taken into account in the computation. This systematic error is quite low as discharge and velocity near bed are concerned [2].

For the narrower channel flow, the simulated velocity at the surface tends to the logarithmic law. This behavior can be explained by the boundary layer at the sidewalls. Indeed their influence is sensitive at the centerline and then modifies the vertical profile in the upper part (Fig. 6).

Fig. 5 Velocity profiles obtained for $k = 0, 0.1$ and 0.05 m and for several B/h ratio with the boundary condition BC2

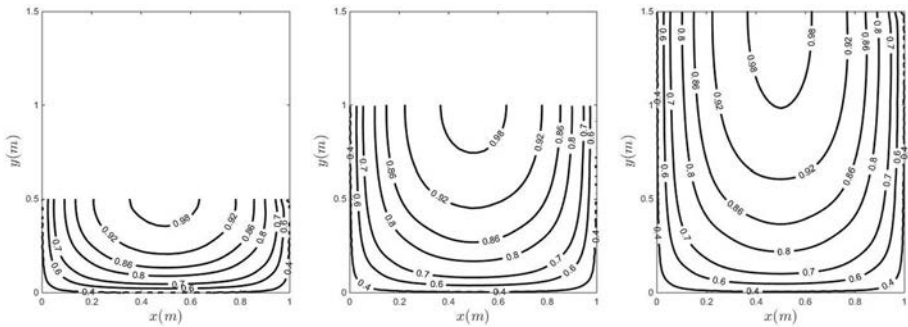
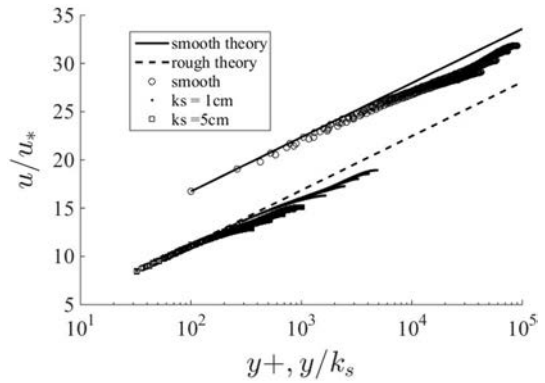


Fig. 6 Isovels obtained for a rectangular channel with smooth condition ($S_f = 0.001$)

For rectangular channel, the repartition of the friction between bed and sidewall has been extensively studied. The most simple way to evaluate this distribution is to consider bisectors of the corners as lines normal to the isovel [15]. The bed shear stress distribution is provided by the ratio of the wetted subarea (Sect. 2.2) delimited by the bed, the bisector and the free surface. For smooth channel Guo and Y. [10] elaborated an analytical solution to obtain the averaged shear stress on sidewall and bed of a rectangular channel. Cacqueray et al. [5] used CFD to improve the results by adding correction factors. These 2 approaches were validated with experiments from literature. The Fig. 7 confirms that the proposed method is also consistent with 3D model and thus with experiments which had validated the CFD results. The additional interest is that the method predicts a local description of the shear stress when the roughness height is not constant. As for velocity field, some discrepancies with the experiments, due to secondary currents, could be expected [17].

4.2 Experiments at IMFT

The computed discharge is compared to our experimental values for the 2 kinds of boundary conditions (BC2 and BC3) on Fig. 8. BC2 and BC3 numerical procedures reproduce correctly the evolution of the stage-discharge relationship since the discharge is well calculated for a given water depth and roughness height. The sensitivity to the roughness height

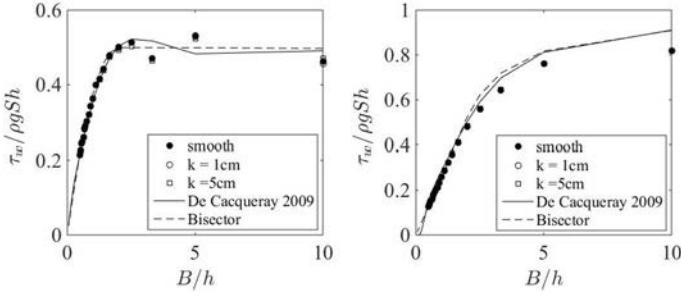


Fig. 7 Bed shear stress distribution for rectangular channel (BC2) on sidewall (left) and on the bed (right) (Numerical results from [5])

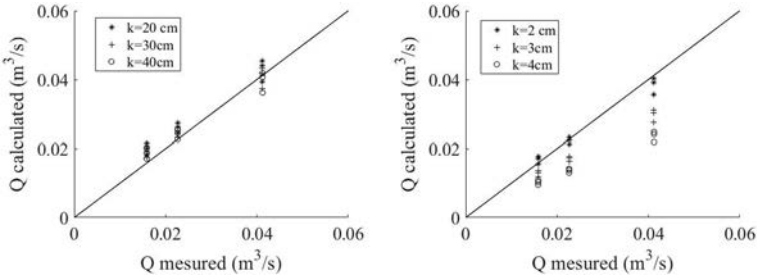


Fig. 8 Comparison of computed and measured discharge as a function of the roughness parameter, for BC2 (left) and BC3 (right)

is illustrated by varying this parameter. The first remark concerns the k value as function of the BC. With BC2, k is largely higher than the mean diameter of roughness even if only one value of $k = 30$ cm is used to compute the stage-discharge relationship for all slopes. The BC3 is more pertinent because $k = 3$ cm provides satisfactory estimate of the discharge (Fig. 8) and corresponds to the range of pebble diameters on the bed.

To validate the method with the present experiments, the surface velocity profiles obtained by LSPTV are compared to the velocity provided by the model (with BC3, $k = 3$ cm) on the Fig. 9. The experimental velocity is obtained by averaging the velocity field in the longitudinal direction. For slope inferior to 1%, the model predicts the velocity surface with a small discrepancy for the entire profile. However the maximum velocity is underestimated at the centerline when slope increases. This gap could be related to secondary currents or the fact that the wake law is not considered in the model. Moreover the experimental velocity field on Fig. 4 presents periodic variation which may be due to free surface interaction. Indeed, in the experiments, the Froude number becomes greater than 0.5 when the slope is superior to 1%.

4.3 Experiments from Kean et al. [14]

To emphasize the advantage of a better boundary formulation in a natural flow, the experiments from Kean et al. [14] are also taken into consideration. The lateral distribution of roughness is the one given by Kean et al. [14]. In particular, the boulder diameter

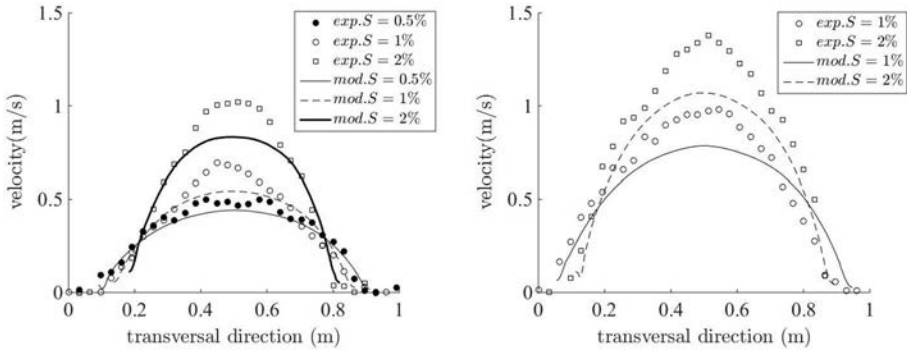


Fig. 9 Transverse profile of longitudinal velocity from experiments and proposed model for $Q = 20$ l/s (left) and $Q = 50$ l/s (right) at the free surface

is 4.5 cm on the floodplain. The experimental data reveals the effect of the roughness height on the boundary layer and above large boulders (Fig. 10).

The computed velocity fields with BC2 and BC3 are in good agreement with those obtained by Kean et al. [14]. The same differences with experiments are observed and are attributed by Kean et al. [14] to secondary currents found experimentally in the bottom left corner. However the velocity is lower with BC2 and the total discharge is 367 l/s whereas the experimental one is 396 l/s. With BC3, the computed discharge is 400 l/s. It could be stated that the discharge is adequately described by the newly proposed method. But it must be noted that the side walls are smooth which explains the similar results for the 2 boundary conditions.

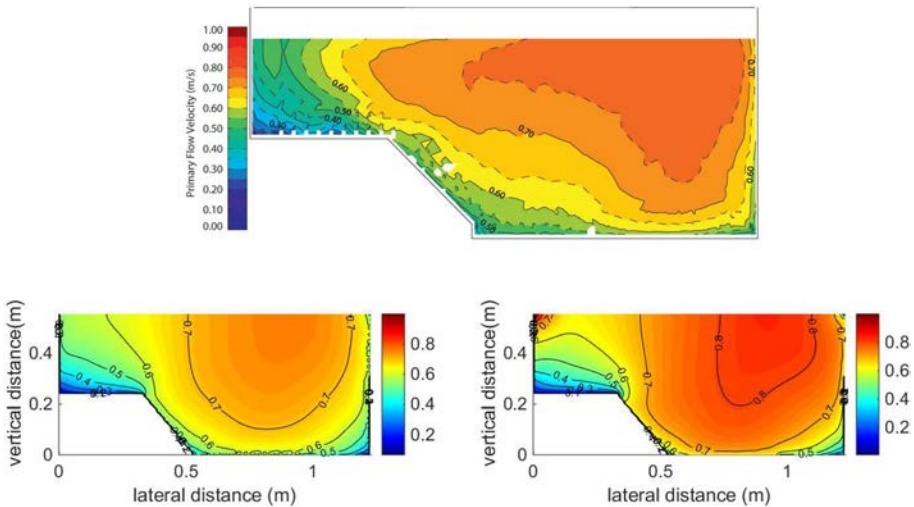


Fig. 10 Velocity field: measured from Kean et al. [14] experiments (top) and computed with $k = 4.5$ cm with BC2 (left) and BC3 (right)

4.4 Experiments from Wang et al. [34]

We described a useful way to obtain quickly the velocity distribution for various cross section shapes and roughness heights. As a consequence, it could help to design structures where areas with low velocity are needed. This objective is essential for fish passage structures as nature-like fishpass or artificial river. With the present method, the detection of low velocity area near the bank is improved, and the influence of the roughness height on this area can be determined in a design process. For small Australian fishes, Wang et al. [34] studied the advantage of adding roughness on culvert bed and sidewalls to enhance the passability of this structure. By reducing velocity near some walls, it appears possible to get a flow slower than the swimming abilities of small fishes. The method is a supplementary tool to assess the modification of the structure conveyance as a function of the roughness. In a first step, the computed velocity is compared to the experiments in a scale model [34]. These experiments were conducted on a rectangular flume with a small roughness on the right sidewall ($k = 0.2$ mm) and a larger roughness on the bed and on the left sidewall ($k = 20$ mm). The bed slope is null and S_f is deduced from the water surface profile.

The Fig. 11 compares experimental velocity with simulated ones with the two kind of boundary conditions. The friction slope is deduced from the experimental Darcy-friction coefficient $f = 0.07$ [37]. It confirms that the method is pertinent since the predicted discharge is 0.0283 m³/s for BC1+BC2 and $Q = 0.0263$ m³/s for BC2 only ($Q = 0.0255$ m³/s in experiments). With BC1, the non symmetric field due to the smooth wall is visible even if it is overestimated. The k^+ value is between 11 and 20 which is the limit for smooth wall. Then the difference could be due to the boundary condition and new calculations are performed with BC3 for all walls. This condition is better suited for prediction of the experiments (Table 2). Although a difference exists in the upper part of the field between experiments and model, our results are consistent with the CFD simulation from Zhang and Chanson [37] computed with similar roughness height. This condition is therefore used for the following comparison (Figs. 12 and 13). It should be mentioned that the hydraulic roughness from Zhang and Chanson [37] has been kept to assess numerical methods. However it would have been possible to calibrate these values since law friction differs. Therefore, the discrepancy between numerical procedure and experiments would decrease significantly.

For the cases with the larger discharge, the method slightly overestimates the flow-rate ($Q \approx 0.059$ m³/s against $Q = 0.055$ m³/s in experiments cf. Table 2). The value f of the roughness description can explain it and k should be calibrated. This adjustment could be due to the roughness shape different from spherical elements corresponding to the BC2 condition.

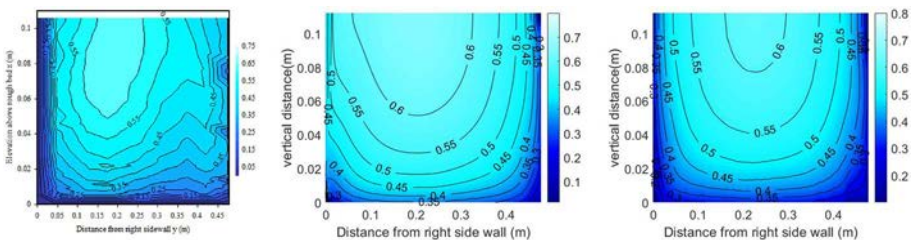


Fig. 11 Experimental velocity fields from Wang et al. [34] for $h = 0.12$ m (left), simulation with a BC1 + BC2 (center) and only BC2 (right)

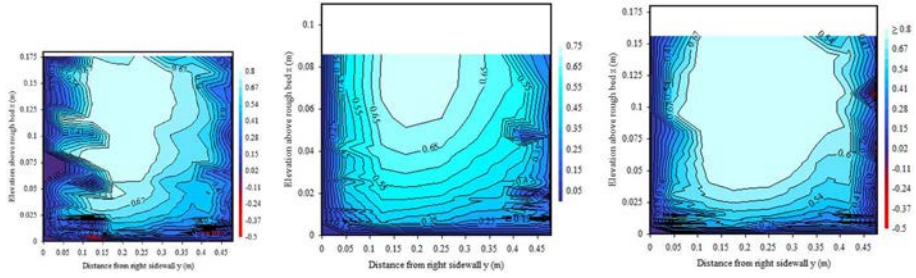


Fig. 12 Experimental velocity fields from Wang et al. [34] for $h = 0.175$ m and $Q = 0.0556$ l/s (left), $h = 0.085$ m, and $Q = 0.0261$ l/s (center) and $h = 0.155$ m and $Q = 0.0556$ l/s (right)

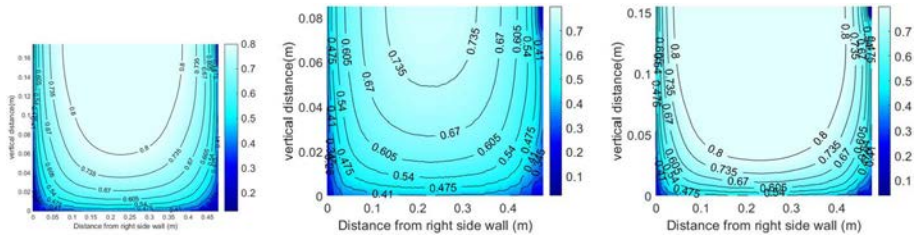


Fig. 13 Computed velocity fields from Zhang and Chanson [37] for $h = 0.175$ m and $Q = 0.0556$ l/s (left), $h = 0.085$ m, and $Q = 0.0261$ l/s (center) and $h = 0.155$ m and $Q = 0.0556$ l/s (right)

Table 2 Velocity distribution in a culvert cross section

	Q (m^3/s)	h (m)	U_{mean} m/s	U_{max} m/s	$U < U_{mean}$ (%)
Wang et al. [34]	0.261	0.129	0.423	0.755	45
Model (BC3)	0.256	0.129	0.42	0.71	47.8
Wang et al. [34]	0.0556	0.1743	0.667	0.957	45
Model (BC3)	0.055	0.1743	0.665	1.11	47

To evaluate the relevance of rough sidewalls, the percentage of wetted areas where the velocity is low is measured. It could be noticed that this percentage is almost constant for a given water depth whatever the discharge. The simulated area where $U < U_{mean}$ is in agreement with the experiments (Table 2). The simulation tends to underestimate the area for threshold velocity lower than U_{mean} (i.e $0.25 U_{mean}$) but it could be due to the difficulty to measure and simulate this close wall region.

5 Implication for environmental applications

In comparison with a CFD calculation the present numerical procedure has several advantages. It could be easily adapted to complex cross section shape, the wall law can be easily modified and the number of parameters is reduced. But the main benefit is the computational cost because only few seconds are needed for a river cross section. Therefore the

Fig. 14 Velocity distribution with the Cassan et al. [3] friction law for $Q = 15.8, 22.3$ and 41.2 l/s (BC3 and $k = 0.03$ m)

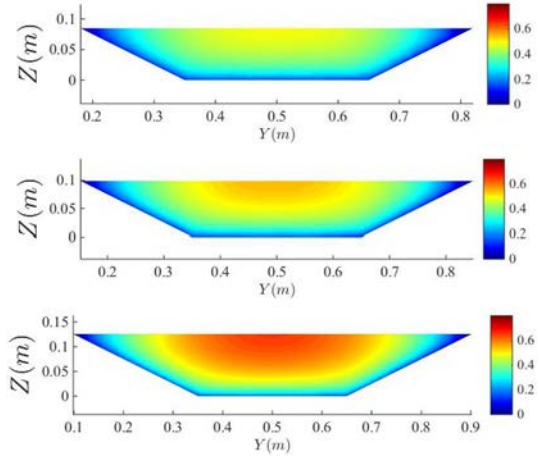


Table 3 Discharge from numerical methods (BC3, $k = 3$ cm) and PTV measurements

	Exp 1	Exp 2	Exp 3	Exp 4	Exp 5
S (%)	0.5	1	1	2	2
h (m)	0.121	0.108	0.149	0.12	0.085
Q measured (l/s) (flowmeter)	20	20	50	50	20
Q estimated with PTV (l/s)	22	20.6	47.7	47.1	22.8

procedure is particularly suitable for environmental applications where the knowledge of the velocity field is necessary. We provide here examples for which the procedure can bring quick solution for restoration, design or measurement issues.

5.1 Hydrodynamic of low submergence flow

The Fig. 14 presents the interest of the method to predict the area where the velocity may be low (see previous part about culvert passage). Indeed this bank zone is potentially relevant for fish spawning and ecological functions in a real river.

All 1D models can be post-treated with this method, then it could be used to evaluate the variation of velocity and sediment transport for long river. It may be a tool for diagnostic of aquatic habitat and river restoration for existing models. The knowledge of turbulent viscosity also helps to compute transversal or vertical transfer of suspended load or pollutant. Moreover the integration of Eq. 3 is consistent with the energy equation on which most 1D models are based. Incorporating this method in a 1D model could improve the precision of the model by computing the head loss with various friction laws (*e.g* BC3).

5.2 Discharge from LSPTV measurements

Although the experimental and computed velocities do not totally agree for our experiments, the total discharge predicted by the model is similar to the experimental one. The maximal error is 10% (Table 3). As a consequence, the method can be coupled with LSPTV measurements to extrapolate the total velocity field. The ratio between the velocity

surface and the averaged velocity can be known with more accuracy for each LSPTV measurements. Thanks to the low computation time, the procedure can also be used for statistical study which would give this velocity ratio as a function of cross section, water depth or roughness.

5.3 Design of real scale fish passage

For a design process of fish passages, the method allows obtaining results at a larger scale and with different roughness. Then the compromise between large low velocity area and sufficient hydraulic conveyance can be found. It is a complementary tool to design guidelines proposed by Leng et al. [18].

The Fig. 15 represents the isovel obtained in a real culvert (2 m wide, $S_f = 0.1\%$) with a roughness of the left sidewall of 2 mm (concrete) and roughness of the bed and other sidewalls with $k = 5, 10$ and 20 cm. These k roughness values are very large but it is an equivalent roughness size (related to the chosen friction law) that could be representative of specific macro-roughness.

The increase of the roughness clearly reduces the velocity and then the conveyance. The difference between the smallest and the largest roughness is not sufficient to exhibit a non symmetric velocity field except in the right bottom corner where velocity is reduced. Thanks to the method, it is possible to provide the stage-discharge relationship as a function of roughness and waterdepth. As a consequence the method can be used for the design of other kinds of fish pass as artificial river or rock ramp.

5.4 Morphodynamic

The forces exerted on banks can have a non uniform lateral distribution which has an impact on the associated erosion. For the experiments of Kean et al. [14], the wall shear stress is better simulated where the roughness height ($k = 0.8$ mm) is well defined i.e on the main channel bed (Fig. 16). It could be explained by the fact that k is in the range of Nikuradse law application. A discrepancy exists on the aluminum sidewalls which are smooth ($X < 0.35$ and $X > 1.6$), then the transition formula of Ligrani and Moffat [19] may be responsible for the difference. Nevertheless the general trend is almost similar to the measured one. In particular the advantage to distribute the shear stress compared to an averaged value clearly appears. For the present experiments, the Fig. 17 exhibits the same variation from the averaged value. The lower shear stress on the banks can be used to study solid transport and forecast the evolution of bed during floods.

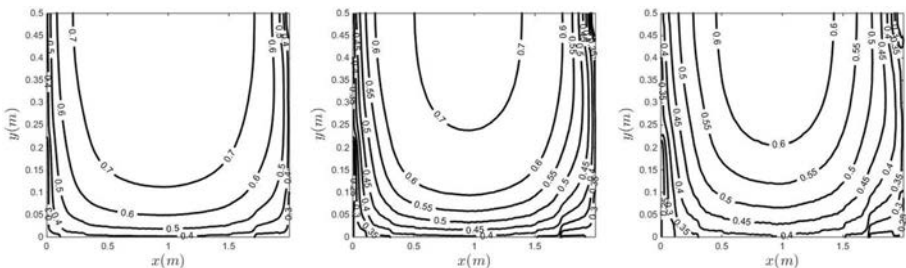


Fig. 15 Isovel for a real scale culvert for roughness of $k = 5, 10$ and 20 cm

Fig. 16 Bed shear stress distribution for experiments from Kean et al. [14]

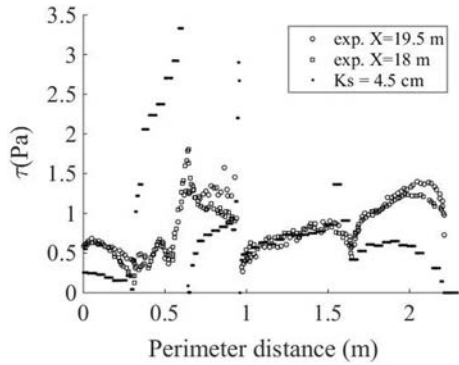
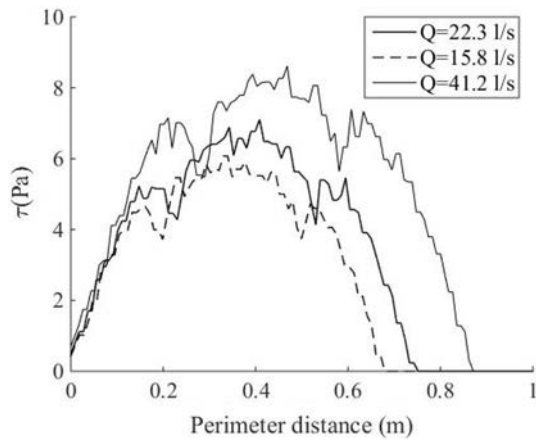


Fig. 17 Bed shear stress distribution with the Cassan et al. [3] friction law (BC3) and $k = 0.15$ m, for $Q = 2, 8$ and 16 m³/s



6 Conclusion

A method to compute the velocity distribution on a cross section has been presented. It is based on the consideration from Kean et al. [14] which predicts the longitudinal velocity with a mixing length turbulent model. The resolution is obtained with a Finite Element Method directly available in Matlab toolbox. Then the method can easily be used as a post processing of all 1D hydraulic models. The main improvement is the explicit description of the boundary condition, especially with the roughness height as a parameter which can be distributed laterally. For large river, the method tends to be similar to the Einstein method and then it is more pertinent for narrow channels. The validation has been performed by comparison with results from Kean et al. [14] and bed shear stress for rectangular and trapezoidal channels. It appears that phenomenon due to secondary currents as dip phenomenon or wake zone are not reproduced by the method. However it is imperative to provide a good estimation of discharge as a function of roughness. Therefore it is justified to use it in design process of hydraulic structure where the flow is unidirectional such as fish passes. For large and narrow open channel flows, the method can be useful to integrate new friction formulae as those developed for macro-roughness or vegetation. Thanks to an ideal river example, the interest of an adapted formulation is demonstrated since the law of

friction has been parametrized with observed roughness size instead of hydraulic roughness varying with hydraulic conditions. Lastly, the method could be useful to extrapolate LSPTV measurements and obtain a more accurate flowrate.

References

1. Cassan L, Laurens P (2016) Design of emergent and submerged rock-ramp fish passes. *Knowl Manag Aquat Ecosyst* 417(45):1–10. <https://doi.org/10.1051/kmae/2016032>
2. Cassan L, Belaud G, Baume Jean-Pierre, Dejean Cyril, Moulin Frederic (2015) Velocity profiles in a real vegetated channel. *Environ Fluid Mech* 15(05):1263–1279
3. Cassan L, Roux H, Garambois PA (2017) A semi-analytical model for the hydraulic resistance due to macro-roughnesses of varying shapes and densities. *Water* 9(9):637. <https://doi.org/10.3390/w9090637>
4. Chiu Chao Lin (1989) Velocity distribution in open channel flow. *J Hydraul Eng* 115(5):576–594
5. De Cacqueray Nicolas, Hargreaves David M, Morvan Hervé P (2009) A computational study of shear stress in smooth rectangular channels. *J Hydraul Res* 47(1):50–57
6. Defina A, Bixio AC (2005) Mean flow and turbulence in vegetated open channel flow. *Water Resour Res* 41:1–12
7. Ducrocq T, Cassan L, Chorda J, Roux H (2017) Flow and drag force around a free surface piercing cylinder for environmental applications. *Environ Fluid Mech* 17(4):629–645
8. Einstein HA, Banks RB (1950) Fluid resistance of composite roughness. *Eos Trans Am Geophys Union* 31(4):603–610
9. Ferguson R (2007) Flow resistance equations for gravel- and boulder-bed streams. *Water Resour Res* 43(5):W05427
10. Guo J, Julien PY (2005) Shear stress in smooth rectangular open-channel flows. *J Hydraul Eng* 131(1):30–37
11. Guo J (2017) Exact procedure for Einstein–Johnson sidewall correction in open channel flow. *J Hydraul Eng* 143(4):06016027
12. Huthoff F, Augustijn DCM, Hulscher SJMH (2007) Analytical solution of the depth-averaged flow velocity in case of submerged rigid cylindrical vegetation. *Water Resour Res* 43(6)
13. Katul G, Poggi D, Ridolfi L (2011) A flow resistance model for assessing the impact of vegetation on flood routing mechanics. *Water Resour Res* 47(8)
14. Kean JW, Kuhnle RA, Smith JD, Alonso CV, Langendoen EJ (2009) Test of a method to calculate near-bank velocity and boundary shear stress. *J Hydraul Eng* 135(7):588–601
15. Keulegan CH (1938) Laws of turbulent flow in open channels. *J Res Natl Bureau Standards* 21:707–740
16. Klopstra D, Barneveld HJ, van Noortwijk JM, van Velzen EH (1997) Analytical model for hydraulic resistance of submerged vegetation. In: *Proceedings of the 27th IAHR congress*, pp 775–780
17. Knight DW, Omran M, Tang X (2007) Modeling depth-averaged velocity and boundary shear in trapezoidal channels with secondary flows. *J Hydraul Eng* 133(1):39–47
18. Leng X, Chanson H, Gordos M, Riches M (2019) Developing cost-effective design guidelines for fish-friendly box culverts, with a focus on small fish. *Environ Manag* 63(6):747–758
19. Ligrani Phillip M, Moffat Robert J (1986) Structure of transitionally rough and fully rough turbulent boundary layers. *J Fluid Mech* 162:69–98
20. Limerinos JT (1970) Determination of the manning coefficient from measured bed roughness in natural channels. *Geological Survey water-supply paper*
21. Luhar M, Rominger J, Nepf H (2008) Interaction between flow, transport and vegetation spatial structure. *Environ Fluid Mech* 8:423–439. <https://doi.org/10.1007/s10652-008-9080-9>
22. Maghrebi Mahmoud F, Rahimpour Majid (2006) Streamwise velocity distribution in irregular shaped channels having composite bed roughness. *Flow Meas Instrum* 17(4):237–245
23. Nepf Heidi M (2012) Hydrodynamics of vegetated channels. *J Hydraul Res* 50(3):262–279
24. Nezu I, Nakagawa H (1993) Turbulence in open-channel flows. *IAHR Monograph Series A. A, Balkema*
25. Nikora N, Nikora V, ODonoghue T (2013) Velocity profiles in vegetated open-channel flows: combined effects of multiple mechanisms. *J Hydraul Eng* 139(10):1021–1032
26. Nikuradse J (1933) Laws of flow in rough pipes (stromungsgesetze in rauhen Rohren) *VDI Forschungsheft* 361. In translation, *NACA Technical Memorandum* 1292, 1950

27. Pagliara S, Chiavaccini P (2006) Flow resistance of rock chutes with protruding boulders. *J Hydraul Eng* 132(6):545–552
28. Patalano A, Garcia CM, Rodrigues A (2017) Rectification of image velocity results (RIVeR): a simple and user-friendly toolbox for large scale water surface particle image velocimetry (PIV) and particle tracking velocimetry (PTV). *Comput Geosci* 109:323–330
29. Raupach MR, Hughes DE, Cleugh HA (2006) Momentum absorption in rough-wall boundary layers with sparse roughness elements in random and clustered distributions. *Boundary Layer Meteorol* 120(2):201–218
30. Rubol S, Ling B, Battiato I (2018) Universal scaling-law for flow resistance over canopies with complex morphology. *Sci Rep* 8(1):4430
31. Talbi Slim H, Soualmia A, Cassan L, Masbernat L (2016) Study of free surface flows in rectangular channel over rough beds. *J Appl Fluid Mech* 9(6):3023–3031
32. Tauro F, Piscopia R, Grimaldi S (2019) PTV-stream: a simplified particle tracking velocimetry framework for stream surface flow monitoring. *Catena* 172:378–386
33. Thornton C, Steven R, Morris Chad E, Fischenich JC (2000) Calculating shear stress at channel-over-bank interfaces in straight channels with vegetated floodplains. *J Hydraul Eng* 126(12):929–936
34. Wang H, Beckingham LK, Johnson CZ, Kiri UR, Chanson H (2016) Interactions between large boundary roughness and high inflow turbulence in open channel: a physical study into turbulence properties to enhance upstream fish migration. Hydraulic Model Report No. CH103/16 School of Civil Engineering, The University of Queensland, Brisbane, Australia. ISBN 978-1-74272-156-9
35. Wang H, Chanson H (2018) Modelling upstream fish passage in standard box culverts: interplay between turbulence, fish kinematics, and energetics. *River Res Appl* 34(3):244–252
36. Yang Shu-Qing, Tan Soon-Keat, Lim Siow-Yong (2004) Velocity distribution and dip-phenomenon in smooth uniform open channel flows. *J Hydraul Eng* 130(12):1179–1186
37. Zhang G, Chanson H (2018) Numerical investigations of box culvert hydrodynamics with smooth, unequally roughened and baffled barrels to enhance upstream fish passage. Tech rept. University of Queensland, School of Civil Engineering